

# Pressure-induced phase transitions of piezoelectric single crystals from the langasite family: $\text{La}_3\text{Nb}_{0.5}\text{Ga}_{5.5}\text{O}_{14}$ and $\text{La}_3\text{Ta}_{0.5}\text{Ga}_{5.5}\text{O}_{14}$

A. Pavlovská,<sup>a</sup> S. Werner,<sup>a\*</sup>  
B. Maximov<sup>b</sup> and B. Mill<sup>c</sup>

<sup>a</sup>Universität München, Institut für Kristallographie und Angewandte Mineralogie, Theresienstrasse 41, D-80333 München, Germany,

<sup>b</sup>Institute of Crystallography, RAS, Leninsky Prospect 59, 117333 Moscow, Russia, and

<sup>c</sup>Moscow State University, 119899 Moscow, Russia

Correspondence e-mail:

stefan.werner@lrz.uni-muenchen.de

Received 6 March 2002

Accepted 10 June 2002

The hydrostatic compression of piezoelectric single crystals of  $\text{La}_3\text{Nb}_{0.5}\text{Ga}_{5.5}\text{O}_{14}$  (LNG) and  $\text{La}_3\text{Ta}_{0.5}\text{Ga}_{5.5}\text{O}_{14}$  (LTG) was studied at pressures of up to 23 GPa in diamond-anvil high-pressure cells using single-crystal X-ray diffraction techniques. The reflection-intensity data for LNG and LTG were collected at pressures of up to 22.8 GPa and 16.7 GPa, respectively. Both compounds show anisotropic behaviour under pressure, which is caused by differences in bonding parallel to the *a* and *c* directions. The compression of strongly rigid structures leads to increasing internal strains and results, at pressures of 12.4 (3) GPa for LNG and 11.7 (3) GPa for LTG, in a transition to lower symmetry. The compressibilities along the *c* axis are almost the same for LNG and LTG through the whole investigated pressure range. In contrast, the pressure dependencies of the *a* axis of these materials are similar only for the initial phase, and the axial compressibilities for the high-pressure polymorphs of LNG and LTG are significantly different to each other. The volume compressibilities of trigonal LNG and LTG (space group *P*321) are about 0.007 GPa<sup>-1</sup>; respective bulk moduli are 145 (3) GPa and 144 (2) GPa. The monoclinic high-pressure phases (space group *A*2) of LNG and LTG show differing compressions, which can be explained by the substitution of Ta<sup>5+</sup> for Nb<sup>5+</sup>. Thus, the bulk moduli for the high-pressure polymorphs of LNG and LTG are  $B_0 = 93$  (2) GPa and  $B_0 = 128$  (12) GPa, respectively. The volume compressibilities of the high-pressure phases at 0.011 GPa<sup>-1</sup> for LNG and 0.008 GPa<sup>-1</sup> for LTG are higher than the initial phases, this effect being more pronounced in the case of LNG.

## 1. Introduction

$\text{La}_3\text{Nb}_{0.5}\text{Ga}_{5.5}\text{O}_{14}$  (LNG) and  $\text{La}_3\text{Ta}_{0.5}\text{Ga}_{5.5}\text{O}_{14}$  (LTG) belong to the set of new promising piezoelectric materials from the langasite family (Mill & Pisarevsky, 2000). There are many publications providing information about the crystal growth, crystal structure at normal conditions, and elastic and acoustic properties of compounds from this family (Takeda *et al.*, 1996; Hornsteiner *et al.*, 1997; Smythe *et al.*, 1999; Bohm *et al.*, 1999). LNG and LTG are taking a leading position in research interest, since they possess the best technical characteristics (moderate–high piezoelectric coupling coefficients, temperature compensation and low acoustic loss). The possible use of these materials as temperature or pressure sensors encourages the investigation of the behaviour of LNG and LTG crystals under extreme conditions (such as pressure *etc.*).

Thus, the aim of this study is to investigate the behaviour of the crystal structure of LNG and LTG at high pressure, in order to characterize the structural stability of these materials under pressure. Accordingly, an investigation of the

compression mechanisms of LNG and LTG at pressures of up to 25 GPa was undertaken using diamond-anvil cell techniques.

LNG and LTG crystallize in the trigonal  $\text{Ca}_3\text{Ga}_2\text{Ge}_4\text{O}_{14}$  structure type with space group  $P321$  (Mill & Pisarevsky, 2000). The crystal structures of these compounds can be described as a mixed framework consisting of layers of tetrahedra sharing corners, which are aligned perpendicular to the crystallographic  $c$  axis, sandwiched between octahedral–decahedral layers (Fig. 1). The tetrahedra are joined to the decahedra and octahedra by shared edges or shared corners, while polyhedra within the octahedral–decahedra layers are joined by shared edges. Most probably, the compression within the tetrahedral layers (the layers of the smallest and most strained polyhedra) will cause a break of high symmetry, with the appropriate reconstruction of tetrahedral layers into the higher-coordinated polyhedra.

Thus, both LNG and LTG are isostructural and isosymmetric. The only difference between the materials is the substitution of  $\text{Ta}^{5+}$  for  $\text{Nb}^{5+}$  ions. This gives rise to a slight deviation in cell and structural parameters. Many compounds with  $\text{Nb}^{5+}$ – $\text{Ta}^{5+}$  substitution (Weitzel, 1976; Malovichko *et al.*, 1987; Voron'ko *et al.*, 1987; Neumann *et al.*, 1992) show, despite having similar material properties, comparative behaviour with distinct differences due to the greater polarization of  $\text{Nb}^{5+}$  ions through neighbouring oxygen anions. This

causes larger distortions of  $\text{NbO}_6$  octahedra compared with  $\text{TaO}_6$  octahedra (Weitzel, 1976). In the case of LNG and LTG, the positions of the central cations of the octahedra are shared by  $\text{Nb}^{5+}$  or  $\text{Ta}^{5+}$  with  $\text{Ga}^{3+}$  in a ratio 1:1. Furthermore, under normal conditions, the characteristic polarization of the oxygen arrangement has not been reported either for LNG or for LTG. One possible conclusion is that the tendency towards a greater polarization of the oxygen arrangements in  $\text{NbO}_6$  compared with that in  $\text{TaO}_6$  may appear after a phase transition to lower symmetry.

## 2. Experimental

The samples of LNG and LTG were prepared from Czochralski-grown single crystals.

The carefully selected single crystals were pressurized using a modified Merrill–Basset diamond-anvil cell (DAC) (Werner *et al.*, 1996). Stainless plates of spring steel (200  $\mu\text{m}$  thick) or wolfram alloy (250  $\mu\text{m}$  thick), with holes eroded by spark erosion, were used as a gasket material. The first series of experiments was performed in the pressure range up to 10 GPa, the upper limit being due to stress imposed on the sample by a solid matrix of the pressure-transmitting medium (methanol, ethanol and water in volume ratios 16:3:1). Four single crystals of each of the title compounds, with different orientations and sizes of approximately 80  $\times$  80  $\times$  50  $\mu\text{m}$ , were used in the subsequent studies. In cooperation with R. Boehler at the Max-Planck-Institut für Chemie (Mainz, Germany) we were able to load the DAC with helium as the hydrostatic pressure medium. This allowed us to reach pressures of up to 23 GPa and above (the investigated pressure range is 3–23 GPa). At pressures above 11 (1) GPa, helium crystallizes. The noble-gas atoms are held together by weak van der Waals forces, which leads to quasi-hydrostatic conditions at high pressures. Even though helium is known to provide close to perfect quasi-hydrostatic conditions at these pressures, to exclude possible systematic errors, two differently oriented tiny crystals of LNG (20  $\times$  30  $\times$  30  $\mu\text{m}$ ) were used in subsequent high-pressure runs.

The pressure calibrations were performed using  $\alpha$ -quartz as an internal pressure standard (Angel *et al.*, 1997) or the ruby-fluorescence method.

The measurements were carried out on an Enraf–Nonius automated four-circle diffractometer (CAD-4) using monochromated  $\text{Mo } K\alpha$  radiation ( $\lambda = 0.7107 \text{ \AA}$ ) and on a Huber diffractometer installed at beamline D3 at HASYLAB ( $0.55 < \lambda < 0.65 \text{ \AA}$ ).

The lattice parameters of trigonal LNG and LTG were measured at various pressures using 16–24 reflections with  $20 < |\theta| < 36^\circ$ , which were centred at four equivalent positions. Reflection-intensity data was collected on LNG and LTG using the  $\omega$ -scan technique. In each data collection, four symmetrically equivalent sets of reflections according to trigonal symmetry were collected. The average value of the FWHM for all reflections (collected by the  $\omega$ -scan technique) of LNG and LTG up to 14 (1) GPa is  $0.008^\circ$ . The reflections broaden with subsequent increases in pressure. Thus, at

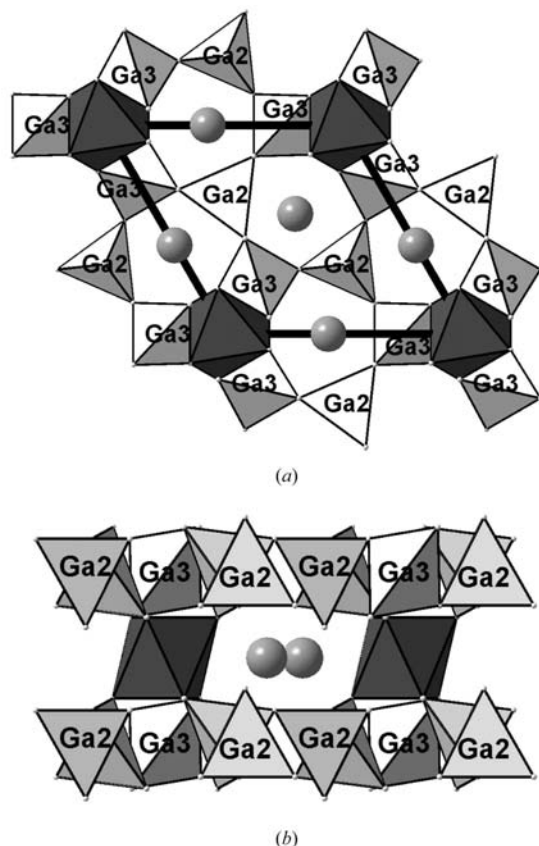


**Figure 1**  
Crystal structure of LNG: (a) *ab* projection; (b) *bc* projection.  $\text{GaO}_4$  and  $\text{Ga/NbO}_6$  polyhedra are shown.

**Table 1**Details of the structure of LNG refined in the trigonal space group  $P321$ .

	Pressure (GPa)							
	0.8	1.8	3.3	4.5	4.8	5.2	6.8	7.8
$\lambda$ (Å)	0.7107	0.6503	0.7107	0.6503	5.083	0.7107	0.7107	0.5596
No. of independent reflections	424	403	425	344	759	412	408	400
No. of parameters	39	39	39	30	39	39	39	39
$R(F)$ (%)	3.9	3.3	3	3.3	4.4	3.86	3.1	4.5
$R(F^2)$ (%)	11.02	7.3	8.9	8.9	13.15	12.86	8.00	10.81
Goodness of fit	1.1	0.9	1.0	1.0	1.0	0.9	1.0	1.0

	Pressure (GPa)							
	9.67	9.9	11.7	13.1	15.6	18.5	21.85	22.85
$\lambda$ (Å)	0.5492	0.5492	0.5600	0.5600	0.5492	0.5492	0.5492	0.5492
No. of independent reflections	656	456	508	473	419	305	283	218
No. of parameters	39	39	39	28	38	28	28	28
$R(F)$ (%)	3.87	4.12	3.8	4.5	6.99	9.4	14.9	14.0
$R(F^2)$ (%)	8.86	11.22	11.57	13.08	18.36	24.05	35.60	34.86
Goodness of fit	0.9	1.0	1.0	1.1	1.4	1.7	2.3	2.6

**Table 2**Details of the structure of LTG refined in the trigonal space group  $P321$ .

	Pressure (GPa)							
	0.7	2.3	3	3.3	5.1	6.1	6.64	7.7
$\lambda$ (Å)	0.7107	0.5588	0.5600	0.7107	0.7107	0.7107	0.7107	0.5600
No. of independent reflections	367	412	759	433	438	424	427	449
No. of parameters	39	39	39	39	39	39	28	39
$R(F)$ (%)	4.2	3.96	4.0	3.76	3.36	4.15	3.98	4.7
$R(F^2)$ (%)	9.71	10.69	13.64	10.88	7.38	9.84	10.75	13.90
Goodness of fit	0.9	1.0	1.1	1.0	0.7	0.9	1.0	1.2

	Pressure (GPa)					
	8.15	9.5	11.57	13.2	14.4	16.7
$\lambda$ (Å)	0.7107	0.5600	0.5600	0.5600	0.5600	0.5600
No. of independent reflections	449	426	434	483	450	841
No. of parameters	39	39	39	39	39	28
$R(F)$ (%)	5.46	4.69	4.94	4.6	4.92	8.88
$R(F^2)$ (%)	12.67	12.92	15.00	13.18	15.26	25.73
Goodness of fit	1.2	1.3	1.3	1.2	1.3	1.7

pressures of 17 (2) GPa, the average value of the FWHM for all reflections is  $< 0.1^\circ$  for LNG and  $< 0.03^\circ$  for LTG. At pressures of around 22 (1) GPa, the FWHM of the reflections of LNG reached  $0.26^\circ$ .

Data reduction was performed using the *REDA* program (Wittlinger *et al.*, 1998). Absorption of the crystal was accounted for using *JANA98* (Petrich, 1997). Anomalous atomic-scattering factors and X-ray absorption coefficients were taken from Sasaki (1989) and Sasaki (1990), respectively. Structure refinement was performed using *SHELXL97* (Sheldrick, 1997). Details of the structure refinement of LNG and LTG can be seen in Tables 1 and 2, respectively.<sup>1</sup> For structure refinements of high-pressure phases of LNG and

LTG, the reflection-intensity data were transformed from trigonal to monoclinic symmetry by the following transformation matrix:

$$\begin{pmatrix} 001 \\ 110 \\ \bar{1}10 \end{pmatrix}$$

The details of the refinement, including appropriate twinning following the former triad in trigonal symmetry, are listed in Tables 3 and 4 for LNG and LTG, respectively.

The *VOLCAL* program (Finger, 1971) was used to calculate and describe the polyhedral shape. Two kinds of polyhedral distortion indices were calculated for tetrahedra and octahedra, namely quadratic elongation (QE) and bond angle variance (AV), which are based on values of bond distances and bond angles, respectively.

<sup>1</sup>Supplementary data for this paper are available from the IUCr electronic archives (Reference: SN0021). Services for accessing these data are described at the back of the journal.

**Table 3**

Details of the structure of LNG refined in the monoclinic space group  $A2_1$ .

$\beta$  is assumed to be  $90.0^\circ$ .

	Pressure (GPa)					
	11.7	13.1	15.6	18.5	21.85	22.85
No. of independent reflections	708	661	481	393	341	295
No. of parameters	75	74	74	75	67	67
$R(F)$ (%)	4.0	5.0	6.18	7.8	12.46	12.3
$R(F^2)$ (%)	10.8	12.97	15.44	19.62	29.99	30.00
Goodness of fit	1	1.1	1.2	1.5	2.1	2.4
Twinning (%)	34:32:34	38:31:31	35:37:28	49:37:14	75:11:14	35:40:25

**Table 4**

Details of the structure of LTG refined in the monoclinic space group  $A2_1$ .

$\beta$  is assumed to be  $90.0^\circ$ .

	Pressure (GPa)			
	11.57	13.2	14.4	16.7
No. of independent reflections	667	757	700	1265
No. of parameters	75	75	75	75
$R(F)$ (%)	4.86	4.75	4.6	7.33
$R(F^2)$ (%)	12.30	12.66	13.18	21.23
Goodness of fit	1.22	1.09	1.14	1.50
Twinning (%)	22:31:47	23:31:46	26:37:37	29:33:48

**Table 5**

Zero-pressure compressibilities ( $\beta_0 \times 10^4 \text{ GPa}^{-1}$ ) of the  $a$  and  $c$  axes of LNG and LTG.

Compound	Low-pressure phase		High-pressure phase	
	$a$ axis	$c$ axis	$a$ axis	$c$ axis
LNG	8.70 (18)	6.24 (2)	15.6 (3)	4.21 (3)
LTG	8.91 (16)	6.57 (8)	6.31 (8)	3.74 (7)

### 3. Results and discussion

Our present study includes data on the unit-cell parameters at pressures of up to 22.8 (3) GPa and 16.7 (3) GPa for LNG and LTG, respectively. Intensity data for LNG were collected at 16 pressure levels between 0.8 GPa and 22.8 GPa. For LTG, intensity data were collected at 15 pressure levels between 0.7 GPa and 16.7 GPa. The unit-cell and structural parameters of LNG and LTG under normal conditions were reported by Molchanov *et al.* (2001) and Takeda *et al.* (1997), respectively, and their results are in agreement with this study. Thus, the cell parameters under normal conditions are:

for LNG,  $a_0 = 8.2250$  (7) Å,  $c_0 = 5.1260$  (4) Å;

for LTG,  $a_0 = 8.228$  (2) Å,  $c_0 = 5.124$  (2) Å.

#### 3.1. Low-pressure phases of LNG and LTG

The pressure dependencies of the relative lattice parameters ( $a/a_0$  and  $c/c_0$ ) of LNG and LTG are plotted in Figs. 2 and 3, respectively. To maintain a simple description of these dependencies, it is necessary to divide each data set into two parts. This leads to the assumption of the existence of phase transitions in both cases. The pressure of the phase transition

can be estimated as 12.4 (3) GPa for LNG and 11.7 (3) GPa for LTG.

For comparison of the axial compressibilities of the title compounds, the bulk moduli were obtained by fitting the Birch–Murnaghan equations of state to the data for lattice parameters  $a$  and  $c$  of LNG and LTG under pressure. The related zero-pressure compressibilities of the axes (Angel, 2000) are listed in Table 5. These results indicate that the

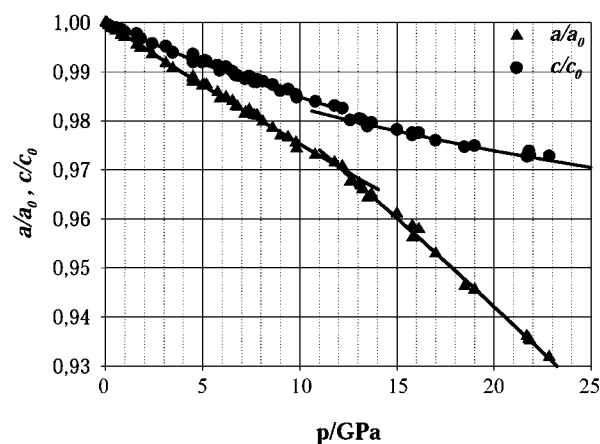


**Figure 2**

The variations of  $a/a_0$  and  $c/c_0$  as functions of pressure for LNG.

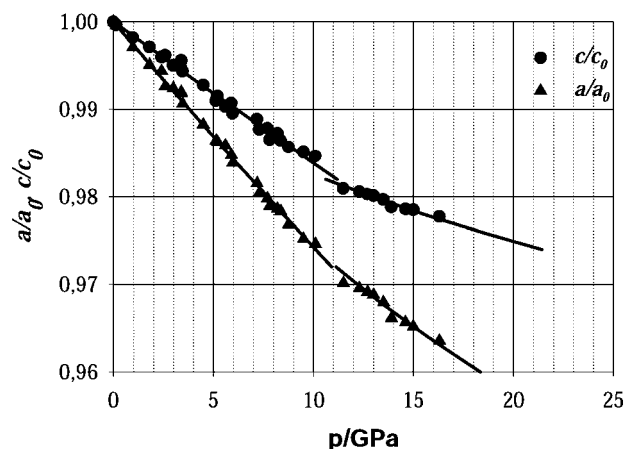


**Figure 3**

The variations of  $a/a_0$  and  $c/c_0$  as functions of pressure for LTG.

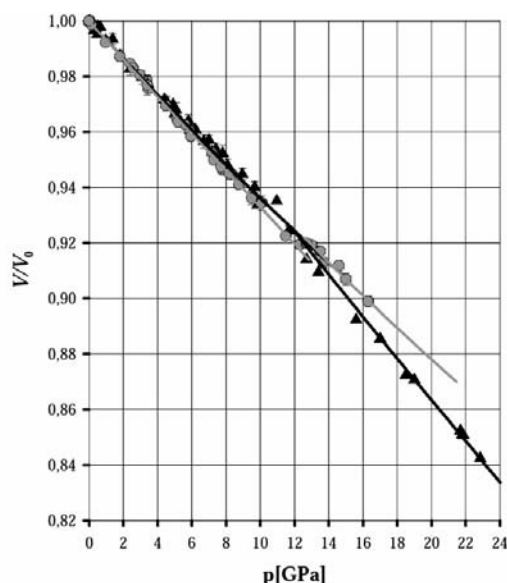
**Table 6**Interatomic distances (Å), polyhedral volumes (Å<sup>3</sup>), quadratic elongation (QE) and angle variance (AV) for polyhedra of LNG.

	Pressure (GPa)							
	0	1.8	3.3	5.2	6.8	7.6	9.67	11.7
<b>La-3e decahedron</b>								
La—O3 × 2	2.413 (3)	2.411 (6)	2.420 (8)	2.392 (14)	2.393 (8)	2.404 (10)	2.392 (9)	2.375 (10)
La—O1 × 2	2.6189 (9)	2.603 (3)	2.598 (7)	2.587 (12)	2.579 (8)	2.554 (7)	2.535 (5)	2.516 (5)
La—O2 × 2	2.464 (2)	2.455 (7)	2.436 (8)	2.418 (16)	2.424 (9)	2.446 (14)	2.410 (11)	2.398 (12)
La—O2' × 2	2.882 (2)	2.877 (6)	2.847 (8)	2.859 (17)	2.843 (11)	2.874 (14)	2.842 (17)	2.827 (17)
Volume	28.67	28.40	28.05	27.7	27.5	27.7	26.96	26.39
<b>Ga-1a octahedron</b>								
Ga—O3 × 6	1.994 (2)	1.988 (5)	1.970 (8)	1.972 (13)	1.977 (9)	1.976 (11)	1.964 (9)	1.964 (10)
Volume	10.2	10.11	9.76	9.7	9.86	9.83	9.67	9.4
QE	1.02	1.02	1.03	1.03	1.03	1.03	1.03	1.03
AV	74.99	79.27	101.95	110.7	100.50	107.8	104.4	111.1
<b>Ga-2d tetrahedron</b>								
Ga—O1	1.809 (3)	1.811 (9)	1.79 (2)	1.77 (3)	1.75 (2)	1.80 (2)	1.780 (14)	1.784 (16)
Ga—O2 × 3	1.840 (2)	1.840 (6)	1.842 (7)	1.846 (15)	1.798 (9)	1.802 (12)	1.813 (10)	1.812 (10)
Volume	3.1	3.08	3.04	3.04	2.84	3.03	2.92	2.9
QE	1.02	1.02	1.02	1.02	1.02	1.01	1.02	1.01
AV	78.23	73.96	90.63	82.3	84.4	56.63	80.76	78
<b>Ga-3f tetrahedron</b>								
Ga—O3 × 2	1.838 (2)	1.831 (6)	1.827 (9)	1.840 (16)	1.815 (10)	1.799 (12)	1.805 (9)	1.812 (11)
Ga—O2 × 2	1.873 (2)	1.859 (6)	1.873 (8)	1.853 (16)	1.865 (9)	1.815 (13)	1.832 (12)	1.830 (10)
Volume	3.11	3.0	3.09	3.07	3.03	2.87	2.91	2.94
QE	1.04	1.04	1.03	1.03	1.03	1.03	1.04	1.04
AV	154.1	158.17	138.99	144.5	153.1	145.5	165.51	176.2

compressibilities along the *c* axis are almost the same for LNG and LTG throughout the investigated pressure range. In contrast, the pressure dependencies of the *a* axes of these materials are similar only for the low-pressure form, whereas the axial compressibilities of high-pressure polymorphs are significantly different in the two compounds. Furthermore, the *a* axis is the most compressible direction for both compounds. This indicates that the compression mechanism of LNG and LTG operates mainly on the *ab* plane. The compressional

anisotropy is typical for a layered structure and can be explained through the differences in bonding characteristics across and within the layers. Thus, the compression within the layers (in the *ab* plane) is achieved mainly through the decreasing volumes and distortions of anion–cation polyhedra. The compression in the *c* direction is more rigid because the polyhedral interconnectivities between the layers (shared edges *etc.*) are less flexible.

In addition, the relative cell volumes  $V/V_0$  of LNG and LTG as functions of pressure are plotted in Fig. 4. The bulk modulus  $K_0$  and pressure derivative  $K'_0$  were obtained by fitting Birch–Murnaghan equations of state to the data obtained. In the pressure range from atmospheric pressure up to 12 GPa, the pressure contractions of LNG and LTG are almost the same and close to linear, demonstrated by the extraordinarily small values of  $K'_0$  [1.4 (8) for LNG and 0.5 (5) for LGT]. Compression is uniform up to this pressure, with calculated bulk moduli of 145 (3) GPa and 144 (2) GPa for LNG and LTG, respectively. Thus, replacing Nb<sup>5+</sup> with Ta<sup>5+</sup> causes almost no difference in the compressibilities of low-pressure phases of LNG and LGT as far as the volume and the axial compressions are concerned.

**Figure 4**

Relative volume compressions of LNG (triangles) and LTG (circles) versus pressure.

### 3.2. Compression mechanism

According to refinements in trigonal space group  $P321$ , the compression mechanisms of crystal structures of LNG and LTG with only several variable positional parameters are quite complex and can be described as follows.

With increasing pressure, the unit-cell volumes of LNG and LTG decrease. Similarly, the distances between ions also

**Table 7**

Interatomic distances (Å), polyhedral volumes (Å<sup>3</sup>), quadratic elongation (QE) and angle variance (AV) for polyhedra of LTG.

	Pressure (GPa)							
	0	2.3	3.3	5.1	7.7	8.15	9.5	11.57
<b>La-3e decahedron</b>								
La—O3	2.428 (7)	2.404 (9)	2.412 (8)	2.403 (8)	2.407 (16)	2.398 (15)	2.403 (12)	2.376 (14)
La—O1	2.618 (3)	2.595 (4)	2.567 (8)	2.569 (5)	2.547 (7)	2.528 (9)	2.516 (6)	2.499 (5)
La—O2	2.464 (6)	2.436 (10)	2.436 (12)	2.411 (8)	2.401 (11)	2.453 (15)	2.45 (2)	2.430 (19)
La—O2'	2.885 (6)	2.868 (9)	2.832 (12)	2.818 (8)	2.82 (2)	2.823 (19)	2.82 (2)	2.77 (2)
Volume	28.85	27.97	27.3	27.23	26.93	26.98	27.02	25.98
<b>Ga-1a octahedron</b>								
Ga—O3	2.007 (6)	1.993 (8)	1.979 (11)	1.993 (7)	1.976 (13)	1.959 (13)	1.959 (11)	1.979 (16)
Volume	10.45	10.17	10.06	10.11	9.80	9.57	9.57	10.02
QE	1.02	1.02	1.03	1.03	1.03	1.03	1.03	1.02
AV	74.23	79.75	88.85	96.91	103.13	103.07	106.59	80.74
<b>Ga-2d tetrahedron</b>								
Ga—O1	1.810 (8)	1.804 (12)	1.88 (2)	1.821 (15)	1.79 (2)	1.86 (3)	1.836 (18)	1.801 (17)
Ga—O2	1.836 (6)	1.830 (9)	1.846 (11)	1.846 (8)	1.826 (16)	1.790 (15)	1.800 (17)	1.793 (16)
Volume	3.06	3.04	3.18	3.08	2.97	2.72	2.97	2.88
QE	1.02	1.02	1.02	1.02	1.02	1.05	1.01	1.02
AV	74.23	83.9	108.35	108.94	74.27	144.34	64.80	110.72
<b>Ga-3f tetrahedron</b>								
Ga—O3	1.819 (6)	1.825 (9)	1.826 (11)	1.812 (8)	1.858 (17)	1.821 (14)	1.800 (13)	1.793 (12)
Ga—O2	1.874 (6)	1.872 (11)	1.864 (11)	1.876 (8)	1.805 (12)	1.838 (17)	1.812 (18)	1.835 (15)
Volume	3.07	3.06	3.1	3.06	2.99	3.1	2.87	2.86
QE	1.03	1.04	1.04	1.03	1.03	1.04	1.03	1.04
AV	158.38	160.44	160.29	155.31	153.3	174.91	150.21	190.41

decrease. The largest cations, La<sup>3+</sup>, are shifted within the *ab* plane (Fig. 5) in order to maximize the distances between the positively charged neighbouring ions Ga<sup>3+</sup> and Nb<sup>5+</sup> (Ta<sup>5+</sup>). The tetrahedrally coordinated Ga<sup>3+</sup> ions are shifted in a similar manner. Because of anion–cation bond shortening, the polyhedra try to rotate and distort. These rotations are hampered because of the shared connectivities of neighbouring polyhedra (including edges). Therefore, compression results mostly in a decrease of the volume of the polyhedra (see also Tables 6 and 7), first with a decrease in the volumes of weakly bonded LaO<sub>8</sub> decahedra (with a predominantly

ionic character of bonding) and Ga/NbO<sub>6</sub> (Ga/TaO<sub>6</sub>) octahedra (partly ionic/covalent types of bonds). The smallest polyhedra (GaO<sub>4</sub> tetrahedra) with apparently covalent-character bonds first try to tilt and distort, because tilting requires much less energy than the shortening of covalent bonds. Nevertheless, the increasing compression (at pressures above 5 GPa) leads to significant shortening of the covalent Ga–O bonds. Moreover, the distortion of the polyhedra tries to increase despite the rigidity that is imposed by two- and threefold-axis laws. The least flexible polyhedra of these structures are 2*d* tetrahedra [the central cations Ga(2)<sup>3+</sup> of these tetrahedra are surrounded by one oxygen atom O1 (at a special 2*d* position) and three oxygen atoms O2 (at a general position) according to the threefold-axis law]. Therefore, because of the lack of flexibility, the strains within Ga2 tetrahedra increase with increasing pressure. This leads to a redistribution of the Ga–O bonds at pressures above 12 (1) GPa. Thus, at pressures above 12 (1) GPa for LNG and LTG, a split position (O21–O22) was determined for O2, which confirmed the existence of phase transitions. These positions (O21–O22) are approximately 0.8 Å apart. With increasing pressure, the distance between O21 and O22 increases (Fig. 6). This phenomenon may be explained as a result of breaking the high symmetry of the crystal structure of LNG and LTG, probably taking away the threefold axes.

It may be concluded that under elevated pressure internal strains increase within the crystal structure of LNG or LTG because the flexibility is very limited. This leads to a phase transition during which the crystal structure of LNG or LTG turns from higher to lower symmetry. This enables a further

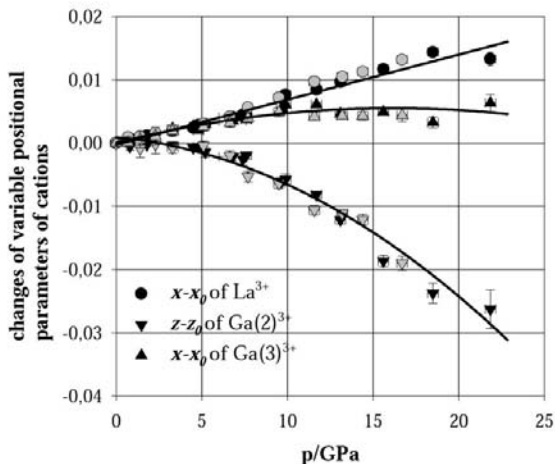


**Figure 5**

Changes of variable coordinates of the cations *versus* pressure of trigonal LNG (black symbols) and LTG (grey symbols).

increase of the compression capability within the structure of LNG or LTG. Thus, at pressures of about 12 (1) GPa, the transformation to a low-symmetry form of higher distortion occurs, which involves more degrees of freedom for subsequent compression.

### 3.3. High-pressure phases of LNG and LTG

For refinements of the structure of high-pressure polymorphs of LNG and LTG, space groups  $P3$  and  $C2$  were tested. These are the maximal non-isomorphic subgroups for space group  $P321$  according to the *International Tables for Crystallography* (1989). The refinement of the crystal structures of LNG or LTG in the space group  $P3$  did not yield satisfying results; furthermore, the split position of O2 was not resolved. The following determination in monoclinic symmetry was made according to Maximov & Mill (2002). It was reported that the crystal structure of another member of the langasite family ( $\text{La}_3\text{Sb}_7\text{Zn}_3\text{Ge}_2\text{O}_{14}$ , LSZG) refined in monoclinic space group  $A2$ . Subsequent refinement of the crystal structure of LNG and LTG in monoclinic symmetry (space group  $A2$ ) allowed us to improve the  $R$  factor and, in contrast to the attempts for refinement in  $P3$ , no split positions for O2 were observed.

The crystal structure of the high-pressure phases of LNG and LTG reveals, as expected, a pseudo-trigonal nature. Thus, the atomic positions of cations refined in the monoclinic space group  $A2$  deviate only within the experimental errors from those refined in trigonal space group  $P321$ . On the other hand, the O-atom positions obtained from these refinements are significantly different.

The lattice parameters of LNG and LGT were found to obey trigonal symmetry within the experimental errors through the whole pressure range. Furthermore, the FWHM of the reflections does not show significant changes up to 14 (1) GPa; the broadening increases with a further increase in pressure. This can be explained by deviations of the  $\beta$  angle from  $90^\circ$  and/or deviations from  $a = b$  in monoclinic domains,

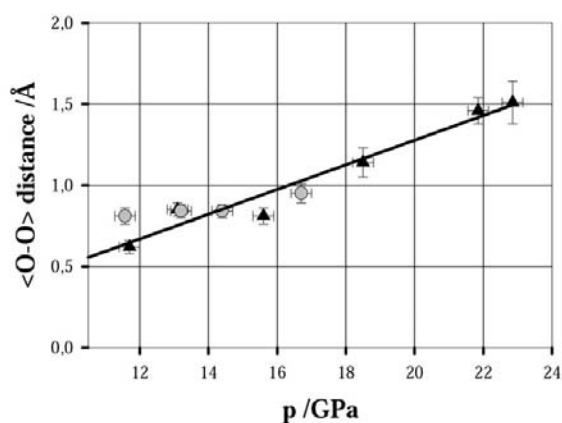


**Figure 6**  
Distance O21—O22 in split position versus pressure for LNG (triangles) and LTG (circles) refined in space group  $P321$ .

which have  $\beta \simeq 90^\circ$  at pressures right above the transition from trigonal to monoclinic symmetry. A broadening of reflection profiles due to non-hydrostatic conditions can be excluded, as the same broadening effect was observed for three single crystals (two LNG crystals and one LTG) with totally different orientations (Pavlovská *et al.*, 2002). Therefore, the monoclinic angle was set to  $\beta = 90^\circ$  in both cases.

In addition, the bulk moduli  $K_0$ , pressure derivatives  $K'_0$  and hypothetical  $V_0$  for the high-pressure phases of LNG and LTG were obtained by fitting Birch–Murnaghan equations of state. Thus, the calculated volume of the high-pressure phase of LNG at room pressure and temperature is  $313$  (6)  $\text{\AA}^3$  and its bulk modulus is  $93$  (2) GPa [ $K'_0 = 1.9$  (9)]. In the case of LTG, fitting results in large errors for  $K_0$  and  $K'_0$  due to the small number of data points and narrow investigated pressure range compared with the case of LNG. With respect to the similarity of the crystal structures of LNG and LTG, the derivative of the bulk modulus ( $K'_0$ ) for the high-pressure phase of LTG was constrained to 1.9 times the value of the high-pressure polymorph of LNG (Angel, 2000). The hypothetical  $V_0$  of the high-pressure phase of LTG stays, within the uncertainty [0.9 (8)%], close to the value for the low-pressure phase of LTG ( $V_0 = 300.41$   $\text{\AA}^3$ ).

Thus, the compressibilities of the title compounds differ only at pressures above the phase transitions. In this pressure range, the high-pressure polymorph of LNG is clearly observed to have a higher compressibility than the low-pressure phase, whereas the compressibility of LTG increases only slightly after the pressure phase transition. Furthermore, whereas the hypothetical  $V_0$  of the high-pressure phase of LNG is 4 (2)% larger than the initial one, the  $V_0$  of the high-pressure phase of LTG remains constant within the error [0.9 (8)%].

In general, an increase in compressibility is a typical indication of polyhedral tilt, in which the high-pressure phase obtains a greater number of tilting degrees of freedom because of its lower symmetry (Hazen & Finger, 1979, 1985; Hazen & Yang, 1997). Thus, because of their high symmetry (two- and threefold axes), the compression of the initial crystal structures of LNG and LTG was strongly restricted. The breaking of the threefold axis of these structures leads to the increased flexibility of the high-pressure polymorph under compression due to the addition of degrees of freedom. The greater increase in compressibility of the high-pressure phase of LNG compared with LTG can be explained by an increased polarization of the oxygen-anion arrangement owing to the presence of  $\text{Nb}^{5+}$  ions, whereas the  $\text{TaO}_6$  octahedra stay almost regular. Fig. 7 shows the  $\text{NbO}_6$  and  $\text{TaO}_6$  polyhedra of high-pressure phases of LNG and LTG. The higher distortion of  $\text{NbO}_6$  octahedra can be clearly seen. Thus, at pressures of around 17.5 (1.0) GPa, the bond distances within  $\text{NbO}_6$  vary from 1.74 (7)  $\text{\AA}$  to 2.12 (6)  $\text{\AA}$ , whereas the Ta—O bond distances are all approximately 1.98 (5)  $\text{\AA}$ , within the errors.

On the other hand, for various compounds, a higher compressibility of the high-pressure phase has been explained by anomalous elasticity (Carpenter & Salje, 1998). Thus, because of elastic softening, the evolution of both lattice

parameters and unit-cell volumes can be affected over a broad range in pressure, showing a typical and more pronounced softening for the low-symmetry form (Karki *et al.*, 1997).

#### 4. Conclusions

The conclusions of this study can be summarized as follows.

The behaviour of LNG and LTG is anisotropic as expected for layered compounds. The *a* axis is the most compressible direction. Consequently, the axial ratio *c/a* increases with pressure. The difference in *a* and *c* compressibilities can be explained in terms of different bond strengths within the polyhedra and different interconnectivities of polyhedra within and between the layers.

The crystal structure of LNG and LTG undergo phase transitions at pressures of 12.4 (3) GPa and 11.7 (3) GPa, respectively. Above these pressures, the structures can be defined as monoclinic.

Like GaPO<sub>4</sub> or  $\alpha$ -quartz (Murashov, 1995; Peters *et al.*, 2000; Haines *et al.*, 2001), the crystal structures of LNG and LTG undergo a phase transition from trigonal to monoclinic. However, the driving forces for these transitions are different. The assumption that the structure comprises tetrahedral chains has provided a suitable model for the crystal structure of the low quartz modifications. The compression of GaPO<sub>4</sub> or  $\alpha$ -quartz leads to tilting and distortion of these tetrahedra. The existence of octahedra and decahedra that share their edges and corners with neighbouring tetrahedra leads to the difference between compression mechanisms of the crystal structures of LNG or LTG and GaPO<sub>4</sub> or  $\alpha$ -quartz. Thus, the compressions of LNG and LTG are mainly achieved by

decreasing the volumes of the polyhedra. The tilting and distortion of the polyhedra is hampered by the shared interconnectivities and high symmetry. This leads to increasing internal strains (especially within the layers of GaO<sub>4</sub> tetrahedra with atomic bonding). Finally, this results in breakage of the high symmetry of the crystal structures of LNG and LTG.

Significant differences in the behaviour of the title compounds under pressure are observed only for the high-pressure phases. The compressibility of the high-pressure phase of LNG is significantly higher than that of the low-pressure polymorph, whereas the compressibility of LTG only slightly increases after the pressure phase transition. This phenomenon can be explained by the greater distortion of NbO<sub>6</sub> compared with that of TaO<sub>6</sub>, which is due to the higher polarization of the oxygen arrangement by Nb<sup>5+</sup>. On further increase of pressure (above 22 GPa), compression of the monoclinic structure of LNG can lead to even more dramatic changes in the crystal structure, with changes in the coordination number most likely for the Ga<sup>3+</sup> cations. It is likely that under higher pressures a similar process will take place in LTG.

The authors are very grateful to Dr R. Boehler (Max-Planck-Institut für Chemie, Mainz, Germany) for the opportunity to load the DAC with Xe and He and for cooperation. Financial support by DFG (WE 2149-3) and FCI (700 372) is gratefully acknowledged.

#### References

- Angel, R. J. (2000). *Rev. Mineral. Geochem.* **39**, 89–91.  
 Angel, R. J., Allan, D. R., Miletich, R. & Finger, L. W. (1997). *J. Appl. Cryst.* **30**, 461–466.  
 Bohm, J., Heimann, R. B., Hengst, M., Roewer, R. & Schindler, J. (1999). *J. Cryst. Growth*, **204**, 128–136.  
 Carpenter, M. A. & Salje, K. H. (1998). *Eur. J. Mineral.* **10**, 693–812.  
 Finger, L. W. (1971). *VOLCAL*. Carnegie Institute of Washington, Geophysics Laboratory, Washington DC, USA.  
 Haines, J., Leger, M., Gorelli, F. & Hanfland, M. (2001). *Phys. Rev. Lett.* **87**, 155503/1–155503/4.  
 Hazen, M. & Yang, H. (1997). *Science*, **277**, 1965–1967.  
 Hazen, R. M. & Finger, L. W. (1979). *Phase Transit.* **1**, 1–22.  
 Hazen, R. M. & Finger, L. W. (1985). *Sci. Am.* **252**, 84–91.  
 Hornsteiner, J., Born, E. & Riha, H. (1997). *Phys. Status Solidi A*, **R3**, 163.  
 Karki, B. B., Stixrude, L. & Crain, J. (1997). *Geophys. Lett.* **24**, 3269–3272.  
 Malovichko, G., Grachev, V. & Bykov, I. (1987). *Sov. Phys. Solid State*, **29**, 244–246.  
 Maximov, B. A. & Mill, B. V. (2002). *Kristallografiya*. Submitted.  
 Mill, B. V. & Pisarevsky, Y. V. (2000). *IEEE/EIA International Frequency Control Symposium*, pp. 133–148.  
 Molchanov, V. N., Maksimov, B. N., Kondakov, A. F., Chernaya, T. S., Pisarevsky, Yu. V. & Simonov, M. I. (2001). *Pis'ma Zh. Eksp. Teor. Fiz.* **74**, 244–247.  
 Murashov, V. V. (1995). *Phys. Rev. B*, **53**, 107–110.  
 Neumann, T., Scharfschwerdt, C. & Neumann, M. (1992). *Phys. Rev. B*, **46**, 10623–10628.  
 Pavlovskaya, A., Werner, S. & Boehler, R. (2002). *Z. Kristallogr.* In the press.  
 Peters, M. J., Grimsditch, M. & Polian, A. (2000). *Solid State Commun.* **114**, 335–340.

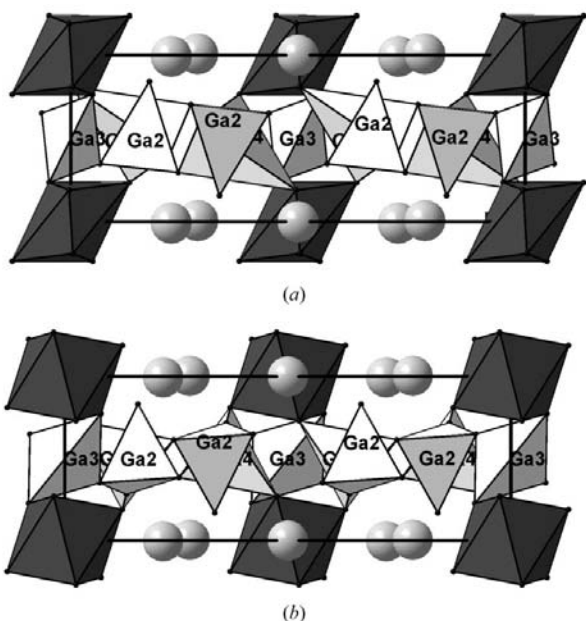


**Figure 7**  
 Projection of the monoclinic unit cell along the *b* axis. The GaO<sub>4</sub> and Ga/NbO<sub>6</sub> or Ga/TaO<sub>6</sub> polyhedra are shown: (a) crystal structure of LNG at pressure 18.5 (3) GPa; (b) crystal structure of LTG at pressure 16.7 (3) GPa.

- Petrichek, V. (1997). *JANA98*. Crystallographic Computing System, Institute of Physics, Academy of Sciences, Praha, Czech Republic.
- Sasaki, S. (1989). KEK Report 88-14, 1-136. KEK, Tsukuba, Japan.
- Sasaki, S. (1990). KEK Report 90-16, 1-143. KEK, Tsukuba, Japan.
- Sheldrick, G. (1997). *SHELX97*. University of Göttingen, Germany.
- Smythe, R. C., Helmbold, R. C., Hague, G. E. & Snow, K. A. (1999). *IEEE International Frequency Control Symposium*, pp. 816-820.
- Takeda, H., Shimamura, K., Koho, T. & Fukuda, T. (1996). *J. Cryst. Growth*, **169**, 503-508.
- Takeda, H. K., Sugiyama, K., Inaba, K., Shimamura, T. & Fukuda, T. (1997). *Jpn J. Appl. Phys.* **36**, 919-921.
- Voron'ko, Yu., Kudryavtsev, A. & Osiko, V. (1987). *Sov. Phys. Solid State*, **29**, 771-775.
- Weitzel, H. (1976). *Z. Kristallogr.* **144**, 238-258.
- Werner, S., Kim-Zajonz, J., Wittlinger, J. & Schulz, H. (1996). *Proceedings of the German-Japanese Workshop on the Use of Ultra-Short Wavelength Photons and  $\gamma$ -rays for High-Precision High-Resolution Analysis of Electronic States of Solids*, pp. 26-29. HASYLAB, Germany.
- Wittlinger, J., Werner, S. & Schulz, H. (1998). *Acta Cryst.* **B54**, 714-721.